Method Evaluation of Liquid Biopsy Proteomics for Limited Plasma Volume

Authors

Ryo Takahashi, Florian Prodinger, and Akiko Matsui

Correspondence

ryo_2.takahashi@boehringer-ingelheim.com

In Brief

Using only 20 µl of rat plasma, we demonstrate for the first time that Mag-Net achieves superior proteome coverage and high-precision enrichment of extracellular vesicle–associated proteins, outperforming ENRICH-iST. This enhanced performance enabled more extensive detection of deregulated proteins and pathways in type 2 diabetes model rats. Our results highlight Mag-Net as a particularly powerful small-volume plasma enrichment method for advancing biomarker discovery and non-clinical efficacy and safety evaluation.

Graphical Abstract

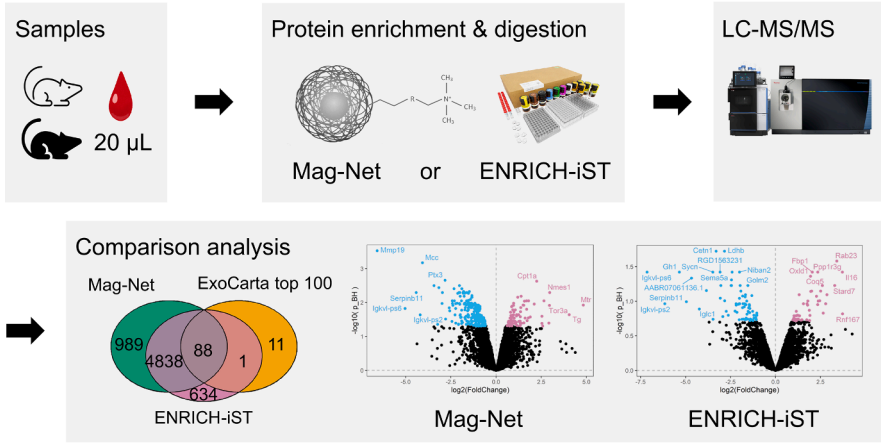

Highlights

- Mag-Net and ENRICH-iST were compared using 20 µl plasma from healthy/diabetic rats.
- More than 5000 proteins were identified by both methods in plasma proteomics.
- Mag-Net highlighted more deregulated proteins/pathways under stricter criteria.
- Elastic fiber formation was found to be downregulated solely by Mag-Net.
- Tissue-specific co-localized proteins were enriched using Mag-Net.

2026, Mol Cell Proteomics *25*(*6*), 101591

https://doi.org/10.1016/j.mcpro.2026.101591

Method Evaluation of Liquid Biopsy Proteomics for Limited Plasma Volume

Ryo Takahashi*, Florian Prodinger, and Akiko Matsui

One of the biggest challenges in plasma proteomics is to reduce the dynamic range of plasma proteins to capture the expression of low-abundance proteins. Although abundant protein depletion and proximity extension assay are widely used for human samples, the application to animal species in non-clinical assessment remains limited. Here, we evaluated the Mag-Net and ENRICH-iST methods using 20 μl of plasma from both healthy and type 2 diabetes model rats. By combining with the optimized LC-MS method, Mag-Net identified more proteins than ENRICH-iST with high precision, although both methods identified over 5000 proteins. Using integrative proteomics and analytical approaches, including extracellular vesicle (EV) database comparison, Gene Ontology analysis, Simple Western, nanoparticle tracking analysis, and contamination assessments, we demonstrated in rat plasma that Mag-Net preferentially enriches EV proteins, whereas ENRICH-iST more evenly captures low-abundance proteins, including EV proteins. Regardless of the protein enrichment method employed, more than half of the tissue-specific proteins were classified as being specific to either the liver or the brain tissues. Whereas, several liver-specific proteins involved in protein-protein interactions, including Proz/Serpina10 and Ambp/Itih1/Itih2, were identified as exhibiting over a ten-fold increase in mean quantification values in the Mag-Net method compared to ENRICH-iST, suggesting enhanced enrichment of protein-protein interaction network. Ingenuity Pathway Analysis identified 219 downregulated and 80 upregulated proteins in the Mag-Net method dataset (fold change $\geq$ 1.5, $p_{BH} \leq 0.05$), and 68 downregulated and 43 upregulated proteins in the ENRICH-iST method dataset (fold change $\geq$ 1.5, $p_{BH} \leq 0.2$). Some significantly downregulated pathways, such as elastic fiber formation, were uniquely identified by the Mag-Net method. This approach was shown to be a powerful tool for investigating deregulated proteins and pathways. Potential applications include biomarker discovery and the assessment of drug efficacy and safety during development.

Plasma proteomics has great potential as a non-invasive liquid biopsy. Since circulating blood contains extracellular vesicles (EVs) and proteins derived from various tissues, approaches that aim to capture tissue-level changes through blood samples are under active investigation (1). This approach is useful not only in clinical trials, but also in non-clinical studies. In non-clinical studies involving commonly used species like mice and rats, quantitative proteomics between control and treated groups offers deeper insights into drug efficacy and toxicity. Although tissues can only be collected at the time of animal sacrifice, blood samples can be obtained from live animals over time.

A major hurdle in plasma proteomics is minimizing the dynamic range of plasma proteins to enable the detection of low-abundance proteins (2). Immunoaffinity depletion of abundant plasma proteins using antibodies has been widely used; however, it has limitations, including limited species applicability, high cost, and the risk of losing target proteins due to the carrier function of abundant plasma proteins (3). Furthermore, non-clinical studies using animals often limit the starting volume of plasma, as the small sample volume must be shared across multiple departments for various analyses. In such a case, less than 50 μl of plasma can typically be used for proteomics.

Therefore, we focused on evaluation of the Mag-Net and ENRICH-iST methods, as both are universally applicable across species and require only a small volume of plasma. The Mag-Net method, which utilizes MagReSyn strong anion exchange (SAX) beads (Resin Biosciences), can enrich a heterogeneous group of membrane-associated particles from plasma (4–7), whereas the ENRICH-iST method (PreOmics) enables physicochemical enrichment of low-abundance proteins (the mechanism has not been publicly disclosed) (8, 9). In this study, we compared the Mag-Net and ENRICH-iST methods using 20 μl of plasma obtained from Zucker Diabetic Fatty (ZDF) rats, an animal model of type 2 diabetes, analyzed by data-independent acquisition (DIA)-MS. Plasma from healthy Sprague-Dawley (SD) rats was also included as a reference. Prior to the main study, the Mag-Net protocol was briefly optimized for a 20 μl plasma volume, as the typical starting volume is 50 μl. We then conducted a comprehensive technical comparison of the Mag-Net and ENRICH-iST methods, evaluating proteome coverage, CV, Gene Ontology (GO) enrichment, and the abundances of known marker proteins. We also investigated the enrichment of tissue-specific

From the Pharmacokinetics and Non-Clinical Safety Department, Nippon Boehringer Ingelheim Co., Ltd, Kobe, Japan
*For correspondence: Ryo Takahashi, ryo_2.takahashi@boehringer-ingelheim.com.

https://doi.org/10.1016/j.mcpro.2026.101591

proteins. In addition, we preliminarily explored the scalability of the plasma proteomics workflow using a short-gradient Orbitrap Astral platform to support high-throughput non-clinical applications.

At the same time, bead-based enrichment approaches are often accompanied by co-enrichment of cellular proteins, necessitating careful evaluation of potential contamination. Accordingly, comparative assessment of bead-based plasma proteomics should consider not only yield and sensitivity, but also the extent and consistency of background cellular contributions. In this study, we systematically compared Mag-Net and ENRICH-iST with respect to enrichment performance and contamination-related characteristics using multiple complementary analytical approaches. Finally, we examined deregulated proteins and pathways in the plasma of ZDF rats compared to healthy control rats.

EXPERIMENTAL PROCEDURES

Experimental Design and Statistical Rationale

In this study, three different individual rats for the control and the dosed group, respectively, were considered as biological replicates and no technical replicates were acquired. To follow 3Rs (replace, reduce, and refine animals used in research) principle, residual rat plasma samples previously purchased in another study were reused for this study. Due to this reason, one of the healthy control samples (SD2), which was repeatedly frozen and thawed 6 times, was selected as an available sample.

Ethics Statement

The animal experiment was conducted in accordance with the Japanese Law and Fundamental Guidelines for Proper Conduct of Animal Experiment and Related Activities in Research Institutions under MHLW on the protection and care of animals used for experimental and other scientific purposes. The experiment was approved by the institutional review board under the study number 2024-06.

Collection and Pretreatment of Rat Plasma Samples

K_2EDTA plasma of healthy control (SD, male, n = 3) and type 2 diabetes (ZDF, male, n = 3) rats were purchased from the Jackson Laboratory Japan, Inc. at the age of 12 weeks. Blood was collected from the abdominal aorta using an 18-gauge needle and centrifuged once at 1750×*g* for 10 min at 4 °C using a swing-out rotor. Plasma was extracted, aliquoted, and stored at −80 °C.

Enrichment of Membrane-Associated Particles by the Mag-Net Method

Plasma was processed by Mag-Net version four protocol (11 Sep 2023) with slight modifications based on the protocol optimization. Briefly, 20 µl of plasma was mixed with 30 µl of Binding Buffer (BB, 100 mM Bis-Tris Propane, pH 6.3, 150 mM NaCl). MagReSyn SAX magnetic microparticles (ReSyn Biosciences) were first equilibrated 2 times in Equilibration/Wash Buffer (WB, 50 mM Bis Tris Propane, pH 6.5, 150 mM NaCl) with gentle agitation and then combined in a 1:4 ratio (beads to sample) with the plasma/BB sample for 30 min at RT. The beads were washed with WB 3 times for 5 min with gentle agitation. The enriched membrane particles were lysed and reduced in 50 mM Tris, pH 8.5/1% SDS/10 mM Tris (2-carboxyethyl) phosphine. Samples were then alkylated with 15 mM iodoacetamide for 30 min at RT in the dark. For on-bead precipitation, the samples were adjusted to 70% acetonitrile, mixed, and then incubated for 10 min at RT. The beads were washed 3 times in acetonitrile and 2 times in 70% ethanol for 30 s each on magnet. On-beads digest was performed in 50 µl of 25 mM ammonium bicarbonate with 0.24 µg of trypsin/Lys-C mix (Promega) overnight at 37 °C. Digestion was quenched by adding 10% formic acid and the supernatant was transferred to a new tube using a magnetic separator. Peptide concentration was determined by fluorometric peptide assay (Thermo Fisher Scientific) with an EnSight plate reader (PerkinElmer) after centrifugation at 10,000×*g* for 5 min at 4 °C. The digested peptides were stored at −80 °C until LC-MS/MS analysis.

Enrichment of Low-Abundance Plasma Proteins by the ENRICH-iST Method

Twenty µl of plasma was processed by ENRICH-iST kit according to the manufacturer's protocol (PreOmics). In brief, 25 µl of EN-BEADS was mixed with 200 µl of EN-WASH at 1200 rpm for 1 min at RT using a ThermoMixer (Thermo Fisher Scientific) and the supernatant was discarded using a magnetic stand. Beads were washed two more times and resuspended with 80 µl of EN-BIND. Plasma samples were incubated with the beads at 1200 rpm for 30 min at 30 °C using a ThermoMixer. The supernatant was discarded using a magnetic stand, and 100 µl of EN-BIND was added and shaken by a ThermoMixer at 1200 rpm for 1 min at RT. The supernatant was discarded on a magnetic stand, and the wash step was repeated two more times. Next, 50 µl of LYSE-BCT was added to each tube and incubated at 1200 rpm for 10 min at 95 °C followed by cooling to RT. To digest proteins, 50 µl of DIGEST was added to each tube and incubated at 500 rpm for 1 h at 37 °C. The digestion was stopped by adding 100 µl of STOP solution and then purified using the filter cartridge in the kit. The peptides were eluted twice with 100 µl of ELUTE. The peptides were dried in a speed-vac (Thermo Fisher Scientific) and resuspended in 15 µl of LC-LOAD. Peptide concentration was determined by fluorometric peptide assay (Thermo Fisher Scientific) after centrifugation at 16,000×*g* for 5 min at 4 °C. Digested peptides were stored at −80 °C until LC-MS/MS analysis.

LC-MS/MS Analysis

The digested peptides were analyzed by a Vanquish Neo UHPLC (Thermo Fisher Scientific) system equipped with an Orbitrap Fusion Lumos mass spectrometer (Thermo Fisher Scientific). One µg of peptides were separated on an Aurora Frontier C18, 60 cm × 75 µm, 1.7 µm UHPLC column (IonOpticks) heated to 55 °C at 300 nl/min using a gradient of 2 to 15% eluent B (acetonitrile containing 0.1% (v/v) formic acid) in 64 min, 15 to 23% eluent B in 30 min, and 23 to 32% eluent B in 20 min followed by a 11 min 95% eluent B wash step.

The mass spectra were acquired using DIA in positive ion mode. MS1 spectra were acquired with the following parameters: a resolution of 120,000, a mass range of 420 to 780 *m/z*, automatic gain control target of 250% (1e6 charges) with dynamic injection time. DIA MS2 spectra were acquired with the following parameters: a 6-*m/z* isolation window, a resolution of 50,000, a precursor isolation range of 420 to 780 *m/z*, a fragment mass range of 200–1200 *m/z*, window placement optimization on, normalized automatic gain control target of 2000% (1e6 charges) with dynamic injection time, higher-energy collisional dissociation collision energy of 30%.

MS Data Analysis

The raw data were processed by DIA-NN software (version 1.8.1) (10) with a spectral library generated by DIA-NN in library-free mode. Data were searched against Rat UniProt database (downloaded July 2023, taxonomy ID: 10116, the number of protein entries: 22842) and

a contaminant database (11). This database was concatenated with one composed of all protein sequences in the reversed order. The search parameters were as follows: up to two missed cleavage sites, 7 to 30 peptide length, carbamidomethylation of cysteine residues (+57.021 Da) as static modifications, N-terminal methionine excision (default setting) as variable modification, mass tolerance for precursor and fragment ions: default setting 0.0 (automatic dynamic correction; optimized mass accuracies were shown in Supplemental Table S1), protein names from FASTA for implicit protein grouping, robust LC (high precision) for quantification strategy, and RT-dependent for cross-run normalization. Precursor ions were adjusted to a 1% false discovery rate (FDR). The result.unique_genes_matrix.tsv was used for further analysis.

Statistical Analysis

Contaminants were removed using Perseus (version 1.6.15.0) (12). Proteins that were not identified in at least two out of three samples in any group were removed. Data were log2-transformed, and missing values were imputed from a normal distribution with a downshift of 1.8 and a width of 0.3. Log2-transformed intensities were averaged, and fold change and Benjamini Hochberg corrected *p*-value were calculated in R (version 4.3.1) using *mod.t.test* (MKmisc package, https://github.com/stamats/MKmisc). The GO of identified proteins were assigned with the Database for Annotation, Visualization, and Integrated Discovery (DAVID, conducted Aug 2025) 2021 bioinformatics resources system (13, 14). Deregulated pathways and protein networks were investigated using QIAGEN Ingenuity Pathway Analysis (IPA, conducted Aug 2024) (QIAGEN Inc., https://digitalinsights.qiagen.com/IPA) (15) and Search Tool for the Retrieval of Interacting Genes/Proteins (STRING, conducted Aug 2024) (version 12.0) (16).

Contamination Analysis

According to Korff's study (17), contamination indices were calculated by dividing the summed intensity of cell-specific marker proteins by the summed intensity of all other quantified proteins. Enrichment scores were calculated by dividing the summed intensity of the 30 defined cell-specific marker proteins by the summed intensity of the top 30 most abundant plasma proteins.

Simple Western Analysis

Membrane particles were enriched from 20 µl or 100 µl of plasma and eluted from MagReSyn SAX beads using 50 µl of Elution Buffer (25 mM Bis Tris Propane, pH 6.5, 1 M NaCl, 0.1% Tween 20). Platelet-poor-plasma (PPP) was obtained by subjecting the purchased plasma to an additional centrifuge at 2500×*g* for 15 min at 20 °C using a fixed-angle rotor. After membrane particle, plasma, and PPP samples were individually prepared from each SD and ZDF rat, the remaining sample volumes were pooled and used for protein quantification using Pierce Rapid Gold BCA Protein Assay Kit (Thermo Fisher Scientific). The EV protein markers Cd9, Cd63, Cd81, tumor susceptibility gene 101 protein (Tsg101), flotillin-1 (Flot1), and ALG-2-interacting protein (Alix), as well as abundant plasma proteins albumin (Alb) and apolipoprotein A1 (Apoa1), were measured using a fully automated Jess Simple Western instrument (ProteinSimple, Bio-Techne) according to the manufacturer's protocol.

Plasma and PPP samples were initially diluted approximately 100-fold using 0.1 × sample buffer (ProteinSimple, Bio-Techne), whereas EV samples were not diluted. All samples were then mixed with Triton X-100 (1% final, Sigma-Aldrich) containing cOmplete protease inhibitor cocktail (1 × final, Sigma-Aldrich), kept on ice, and sonicated twice for 10 s. They were incubated with fluorescent 5 × master mix (ProteinSimple, Bio-Techne) containing DTT (ProteinSimple, Bio-Techne) at 70 °C for 5 min for Flot1, Alix, Alb, and Apoa1, and at 37 °C for 10 min for Tsg101, but without DTT at 70 °C for 5 min for Cd9, Cd63, and Cd81. Electrophoresis was performed using a 12–230 kDa Separation Module (SM-W003) on a 25-capillary cartridge with chemiluminescence detection. Rabbit primary antibodies were purchased for Cd9 (proteintech, 20597-1-AP), Cd63 (Boster Biological Technology, A01080-2), Cd81 (proteintech, 27855-1-AP), Tsg101 (proteintech, 28283-1-AP), Flot1 (proteintech, 215571-1-AP), Alix (proteintech, 12422-1-AP), Alb (proteintech, 16475-1-AP), and Apoa1 (Invitrogen, PA5-29557) and diluted with Antibody Diluent II (ProteinSimple, Bio-Techne) according to the manufacturer's instructions at 1:100, 1:10, 1:10, 1:250, 1:500, 1:50, 1:1250, 1:1250, respectively. Corresponding rabbit secondary antibodies (ProteinSimple, Bio-Techne) were used. Lyophilized exosomes from Plasma of Healthy donors (HansaBioMed) were used as a control sample to validate the workflow. Data analysis was performed using Compass software (version 6.3.0, https://www.bio-techne.com/resources/instrument-software-download-center).

Nanoparticle Tracking Analysis

Membrane particles were prepared from individual SD and ZDF rats and eluted from MagReSyn SAX beads using 100 µl of Elution Buffer (25 mM Bis Tris Propane, pH 6.5, 1 M NaCl, 0.1% Tween 20). The samples were combined and diluted 500-fold with 0.22 µm-filtered 1 × PBS, pH 7.4. The diluted sample was analyzed using the Nanosight Pro (Malvern Panalytical Ltd). Measurement parameters were set as follows: automatic camera and focus setup, laser wavelength 405 nm, sample temperature 21 °C, five captures, flow rate 3 µl/min, capture duration 23.9 s (750 frames), frame rate 31.4046 fps, and camera exposure 31.79 ms. Particle counts were determined using NS XPLORER v1.1.0.6 (Malvern Panalytical Ltd).

RESULTS

Optimization of Mag-Net Protocol

Typical starting volumes of plasma for the ENRICH-iST and Mag-Net methods are 20 µl and 50 µl, respectively. Therefore, prior to their technical comparison, we briefly optimized a Mag-Net protocol for a 20 µl plasma volume using a different LC-MS system with a shorter gradient to accelerate preliminary evaluation (Supplemental Methods & Figures). Protein identification number increased depending on the starting volume of plasma (Fig. 1*A*). Adding protease inhibitor to bind buffer slightly decreased the protein identification number. In the digestion step, an alternate digest buffer of 25 mM Tris-HCl pH 8 instead of ABC buffer was examined to reduce bead adherence to tube walls according to the original protocol, however, it did not improve the protein identifications. Overnight tryptic digestion of 20 µl plasma samples achieved comparable protein identifications to those obtained from 50 µl samples. Analysis of missed tryptic cleavages revealed a correlation between fewer missed cleavages and a higher number of identified proteins (Supplemental Fig. S1). Furthermore, CV for protein abundances across three sample preparation replicates was assessed (Fig. 1*B*). Overnight tryptic digestion of 20 µl plasma samples showed the lowest median CV (6.83%); therefore, this condition was applied in the subsequent main study.

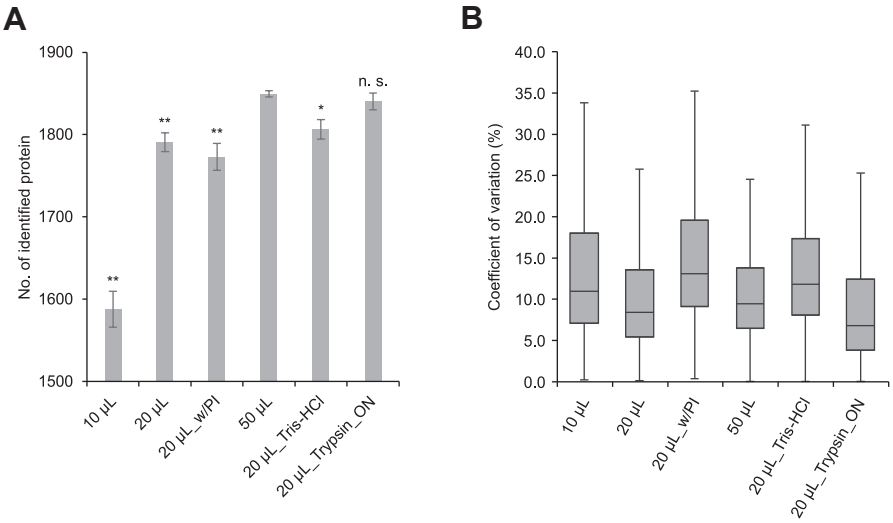

FIG. 1. **Optimization of Mag-Net protocol.** *A,* number of identified proteins of three technical replicates prepared with different conditions (n. s. = not significant; * = p-value < 0.05; ** = p-value < 0.01, determined by a two-sided unpaired Student's t test against 50 µl samples). *B,* CV for protein abundances across three technical replicates prepared with each condition.

Technical Comparison of Mag-Net and ENRICH-iST Methods

Twenty µl of plasma from SD and ZDF rats were processed in triplicate using the Mag-Net and ENRICH-iST methods. After tryptic digestion, the resulting peptides from both workflows were subjected to LC-MS/MS using the same method to ensure a direct comparison. A total of 5915 and 5561 proteins were identified by DIA-MS using the Mag-Net and ENRICH-iST methods, respectively (Fig. 2*A*). A total of 4926 overlapping proteins were identified by both Mag-Net and ENRICH-iST (Fig. 2*A*). The overlap between the identified proteins and the top 100 small EV proteins listed in ExoCarta (Release date: 20 March 2025) (18) was also investigated. Among the top 100 proteins, 88 proteins were commonly identified by both the Mag-Net and ENRICH-iST methods (Fig. 2*A*) (Supplemental Table S2). These results indicate that the identified proteins indeed reflect EV-associated content. The number of identified proteins between SD and ZDF were comparable in both methods (Fig. 2*B*). The CVs of protein quantification values among the three biological replicates were assessed (Fig. 2*C*) using datasets without missing values and prior to imputation. The ENRICH-iST showed similar median CVs of 23.9% and 24.6% for SD and ZDF rats, respectively. Whereas the Mag-Net exhibited lower median CVs of 15.7% and 10.3% for SD and ZDF rats, respectively. To investigate the basis for Mag-Net's higher reproducibility and coverage relative to ENRICH-iST, we evaluated peptide hydrophobicity and digestion performance. Grand average of hydropathy scores (19) were calculated to assess whether peptide loss was biased toward hydrophilic or hydrophobic peptides. Mag-Net identified both hydrophilic and hydrophobic peptides in a balanced manner and in greater numbers than ENRICH-iST (Supplemental Fig. S2). Digestion efficiency was also examined by comparing the average number of missed tryptic cleavages using DIA-NN output (stats.tsv). Mag-Net showed stable values (0.29–0.31), whereas ENRICH-iST exhibited greater variability (0.13–0.22) (Supplemental Table S1). After removing proteins detected in fewer than two out of three replicates, the total number of proteins identified by the Mag-Net and ENRICH-iST methods slightly decreased to 5825 and 5434, respectively (Supplemental Table S1). These numbers of identified proteins exhibited a remarkable increase—approximately eight-fold compared to a previous study using ZDF rat plasma (20).

In principal component analysis (PCA), Mag-Net samples showed clearer clustering within each group compared to ENRICH-iST samples, except for the SD2 sample (Fig. 3). To evaluate the quality of the SD2 sample, which had undergone repeated freeze–thaw cycles, we examined the number of identified proteins among the control samples, the correlation coefficients of protein abundances, and the proteins that strongly contributed to PC2 in the PCA.

Firstly, 92% of the total identified proteins (5362 out of 5858) overlapped among the three biological replicates prepared by the Mag-Net method (Supplemental Fig. S3) (Supplemental Table S3). Besides, 88 proteins of ExoCarta top 100 proteins were detected in all three samples.

Secondly, the correlation coefficients of protein abundances among SD1, SD2, and SD3 prepared by the Mag-Net method were 0.96, 0.97, and 0.97, respectively (Supplemental Fig. S4). These values were comparable to those observed in the ZDF samples (Supplemental Fig. S4) and even slightly higher than those in the ENRICH-iST samples (ZDF1–ZDF2: 0.94; ZDF1–ZDF3: 0.95; ZDF2–ZDF3: 0.96) (Supplemental Fig. S5). These

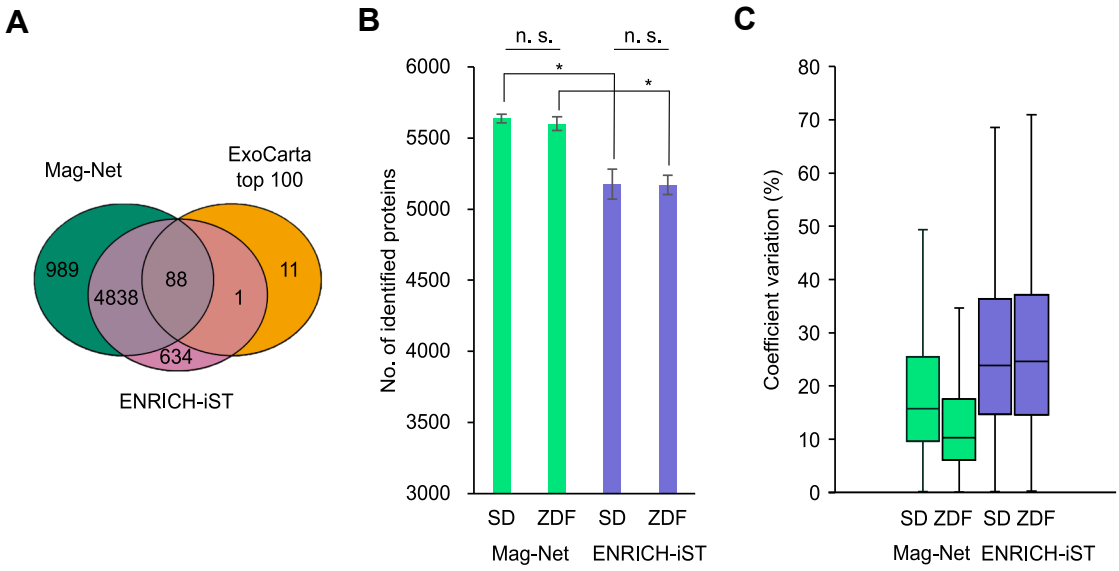

FIG. 2. **Comparison of identified protein number and quantification variability between Mag-Net and ENRICH-iST methods using SD and ZDF rat plasma.** *A,* Venn diagram of ExoCarta top 100 proteins and identified proteins in Mag-Net and ENRICH-iST. *B,* number of identified proteins of three biological replicates in each method (n. s. = not significant; * = p-value < 0.05, determined by a two-sided unpaired Student's t test). *C,* CV for protein abundances across three biological replicates. SD, Sprague-Dawley; ZDF, Zucker Diabetic Fatty.

results indicate that PCA may overestimate differences among control samples because the variables being compared are highly correlated.

Thirdly, the proteins that strongly contributed to PC2 in the PCA were identified, as SD2 was positioned outside the control group cluster in the Mag-Net samples, although PC2 accounted for 19.2%, which was still relatively lower than in ENRICH-iST (PC2: 26.1%) (Fig. 3). A loading plot for PC2 was generated, and the top 10% of proteins (583 proteins) were identified (Supplemental Table S1). If the freeze–thaw cycle affected vesicle integrity and EV purity, the recovery of EV-related proteins could be significantly disrupted in the SD2 sample. Among the top 583 proteins contributing to PC2, only five proteins (Cct2, Ehd1, Eef1g, Rab7a, Vcp) were listed in the ExoCarta top 100 proteins. Of these, only Ehd1 and Rab7a showed changes in SD2 that were more than 1.5-fold higher or lower compared to SD1 and SD3 (Supplemental Fig. S6), suggesting that the overall impact on the EV protein profile was minimal.

Taken together, these results revealed no substantial differences among the control samples and indicate that SD2 is comparable to SD1 and SD3, although a slight impact on EV

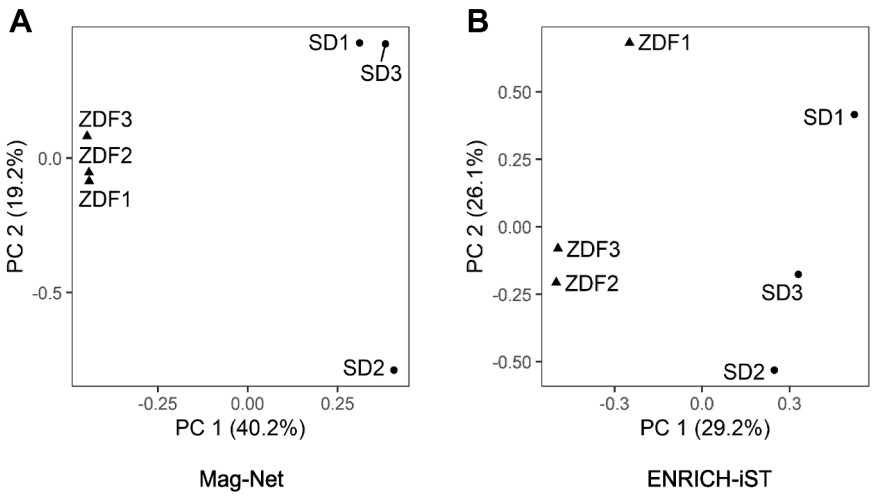

FIG. 3. **PCA of three biological replicates from Mag-Net and ENRICH-iST methods.** The circle and triangle show SD and ZDF samples, respectively. Mag-Net *A,* showed clearer separation among groups than ENRICH-iST *B,* in PCA. Only SD2 rat plasma had been subjected to six freeze-thaw cycles prior to use. SD, Sprague-Dawley; ZDF, Zucker Diabetic Fatty.

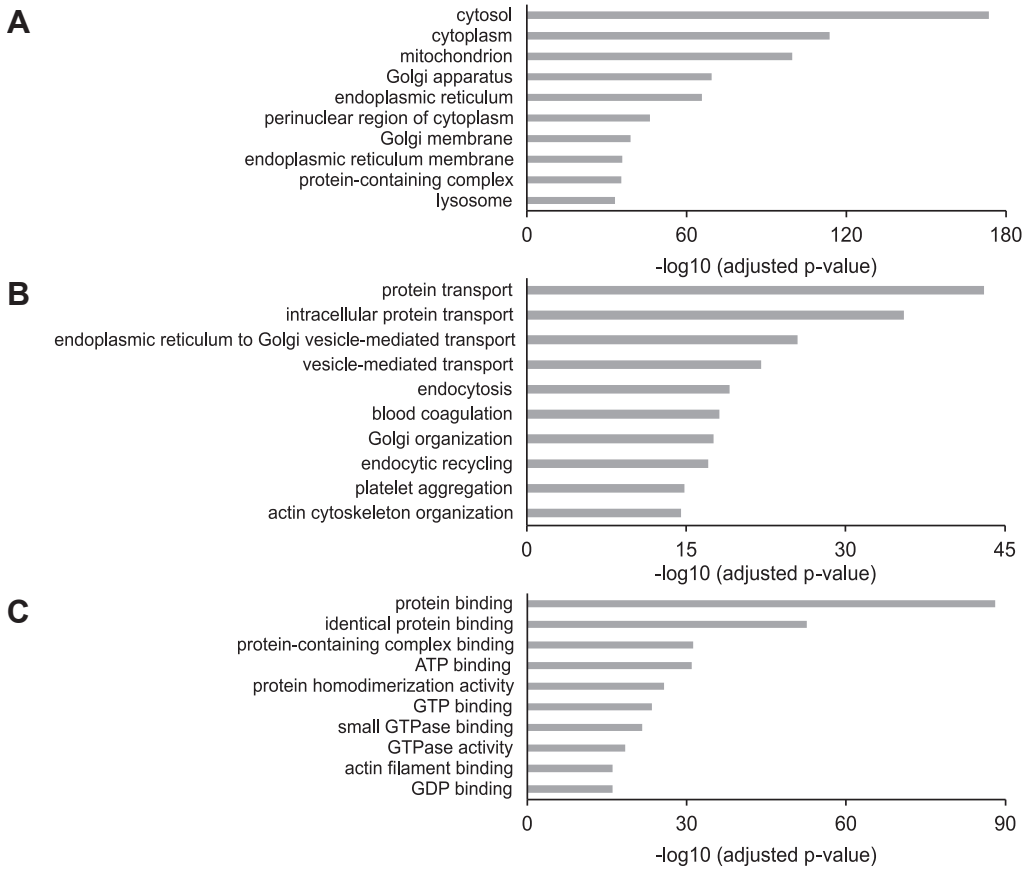

FIG. 4. **GO analysis of proteins commonly identified using Mag-Net and ENRICH-iST.** The top 10 enriched GO terms in the *(A)* cellular component, *(B)* biological process, and *(C)* molecular function categories are represented.

membrane integrity due to repeated freeze–thaw cycles of the SD2 sample cannot be entirely ruled out.

Next, the 4829 proteins commonly identified by both the Mag-Net and ENRICH-iST methods (Supplemental Table S1) were subjected to GO analysis using DAVID (13, 14). The identified proteins showed a broad range of localization in the cellular component category (Fig. 4*A*). Nevertheless, the biological process and the molecular function categories showed enrichment of protein transport (Fig. 4*B*) and protein binding (Fig. 4*C*), respectively. Then, GO analysis was conducted on 996 and 606 proteins exclusively identified by the Mag-Net and ENRICH-iST methods, respectively (Supplemental Table S1). No enrichment was observed for Mag-Net (Supplemental Fig. S7) while extracellular region and extracellular matrix organization were enriched in the ENRICH-iST method under the cellular component and biological process categories, respectively (Supplemental Fig. S8). Subsequently, from the ENRICH-iST-specific protein list (Supplemental Table S1), 146 proteins containing "extracellular" in the GOCC annotation were extracted. When these were highlighted in a relative protein ranking plot, it was revealed that even proteins with moderate expression levels were not identified by the Mag-Net method (Supplemental Fig. S9). Additionally, GO analysis was performed on 1524 proteins with over two-fold higher mean abundance in Mag-Net–processed samples compared to ENRICH-iST–processed samples (Supplemental Table S1), which showed a significant enrichment of the proteasome core complex proteins (Supplemental Fig. S10). Proteasomes encapsulated in EVs have been previously reported (21), and elevated proteasome levels have been described in several diseases such as psoriasis (22), metastatic melanoma (23), and renal cell carcinoma (24). Although proteasomes were not deregulated in ZDF rat samples, the enrichment observed in the Mag-Net workflow suggests that this protocol can capture proteasome-associated EV components.

The abundances of known EV markers such as Cd9 and Cd63, as well as abundant plasma proteins such as Alb and Apoa1, were comparable between Mag-Net and ENRICH-iST samples (Supplemental Fig. S11). To highlight differences in enrichment specificity between the two approaches, relative ranking plots for both Mag-Net and ENRICH-iST datasets, labeling the ExoCarta top 100 proteins were provided (Fig. 5). EV-associated proteins tended to have lower percentile ranks (*i.e.,* closer to the top) in Mag-Net than in ENRICH-iST (median 9.40% *versus* 11.70%; n = 88). Using the criteria $|\Delta\text{percentile}| \geq 0.20$ ($\Delta\text{percentile}$ = Mag-Net_percentile - ENRICH-

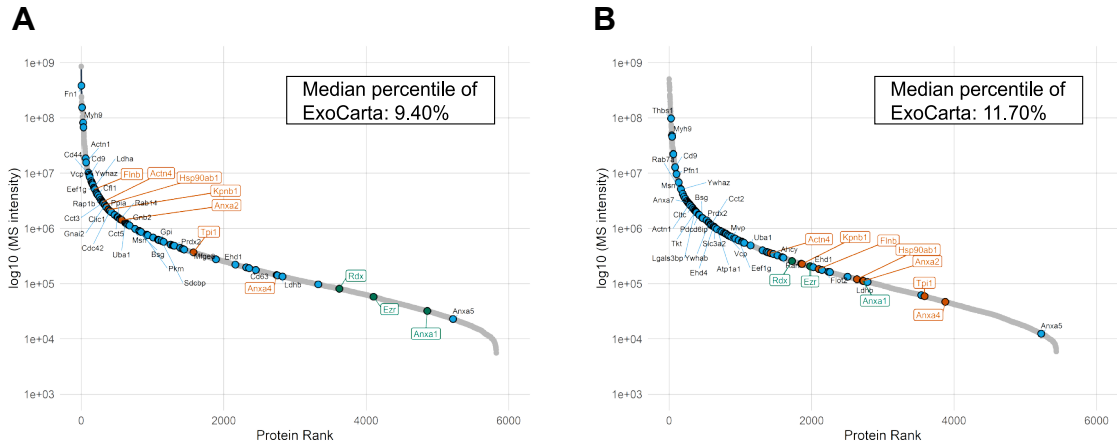

FIG. 5. **Relative ranking plots for Mag-Net and ENRICH-iST, highlighting the ExoCarta top 100 proteins.** *A* and *B*, Mean quantification values of each protein in SD and ZDF rat plasma samples prepared by Mag-Net and ENRICH-iST were used to generate the ranking plot. The median percentile of ExoCarta top 100 proteins in Mag-Net and ENRICH-iST were 9.40% and 11.70%, respectively. Using the criteria $|\Delta\text{percentile}| \geq 0.20$ (Δpercentile = Mag-Net_percentile - ENRICH-iST_percentile), seven proteins (Flnb, Actn4, Hsp90ab1, Kpnb1, Anxa2, Tpi1, Actn4) and three proteins (Rdx, Ezr, Anxa1) were identified as enriched in Mag-Net and ENRICH-iST samples, respectively. SD, Sprague-Dawley; ZDF, Zucker Diabetic Fatty.

iST_percentile), we identified seven proteins (Flnb, Actn4, Hsp90ab1, Kpnb1, Anxa2, Tpi1, Anxa4) enriched in Mag-Net samples and three proteins (Rdx, Ezr, Anxa1) enriched in ENRICH-iST samples (Supplemental Table S1). The protein rankings of Flnb, Actn4, Hsp90ab1, Kpnb1, and Anxa2 in Mag-Net samples were relatively high (189, 298, 329, 381, 567), whereas the rankings of Rdx, Ezr, and Anxa1 in ENRICH-iST samples were moderate (1725, 1978, 2719) (Fig. 5). These results indicate that Mag-Net preferentially enriches EV proteins, whereas ENRICH-iST captures low-abundance proteins, including EV proteins, in a more balanced manner.

Enrichment of tissue-specific proteins was also investigated (Fig. 6*A*). Proteins with at least a four-fold higher expression in the tissue of interest compared to other tissues were defined as tissue-specific proteins in the Human Protein Atlas (HPA, https://www.proteinatlas.org) (25) dataset (3150 proteins, conducted Nov 2024) (Supplemental Table S1). The result identified 359 and 356 proteins in Mag-Net and ENRICH-iST samples, respectively. Several liver-specific proteins involved in protein-protein interactions (PPI), including Proz/Serpina10 and Ambp/Itih1/Itih2, were identified as exhibiting over a ten-fold increase in mean quantification values in the Mag-Net method compared to ENRICH-iST, suggesting enhanced enrichment of PPI network (Fig. 6*B*). Regarding brain-specific proteins (Fig. 6*B*), amyloid precursor-like protein 1 (Aplp1) positive-EVs have been reported as potential biomarkers for the early detection of neurodegenerative diseases (26).

Purity Assessment of Mag-Net and ENRICH-iST Samples

Since bead-based enrichment methods are highly susceptive to contamination from blood cells such as platelets, peripheral blood mononuclear cells (PBMC), and erythrocytes (17), the relative ranking of the top 30 blood cell-specific markers (Supplemental Table S4) was investigated as an initial step. The results showed that the ranking was highest for platelet markers, followed by PBMC and then erythrocyte markers, with platelets being particularly strongly enriched (Fig. 7). While the average median rankings for platelet and PBMC markers were nearly identical between Mag-Net and ENRICH-iST, erythrocyte markers exhibited a noticeable difference, with Mag-Net ranking erythrocyte markers lower (1501) than ENRICH-iST (1078) (Fig. 7) (Supplemental Table S4).

As the next step, we followed the framework proposed by Korff *et al.* (17) to assess potential blood cell-derived contamination. The calculated contamination indices for platelets, PBMC, and erythrocytes were 0.07 to 0.08, 0.007 to 0.008, and 0.005 to 0.006, respectively, in the Mag-Net samples; and were 0.04 to 0.06, 0.005 to 0.008, and 0.003 to 0.006, respectively, in the ENRICH-iST samples (Supplemental Table S4). No outlier samples were detected based on the contamination indices and group-wise comparison of contamination indices revealed no significant differences between SD and ZDF groups (Supplemental Table S4). Furthermore, no significant differences of contamination markers between the groups were identified using the criteria (fold change $\geq$ 1.5, $p_{BH} \leq 0.05$) (Supplemental Table S4), indicating the absence of systematic contamination bias. Given the absence of systematic bias, correlation-based validation using cell-specific marker intensities was not included in this analysis. In contrast, the enrichment scores for platelets, PBMC, and erythrocytes were 0.12 to 0.15, 0.013 to 0.016, and 0.010 to 0.013, respectively, in the Mag-Net samples; and were 0.06 to 0.10, 0.008 to 0.013, and 0.005 to 0.009, respectively, in the ENRICH-iST samples

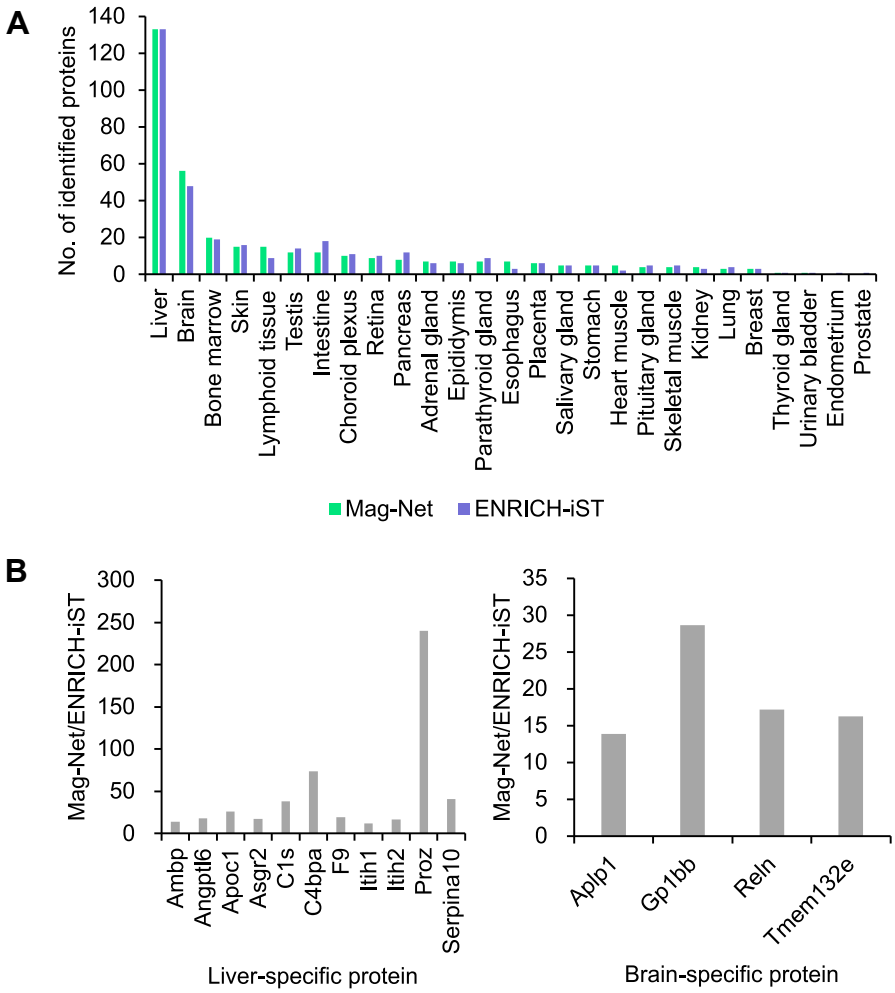

FIG. 6. **Relative ranking plots for Mag-Net and ENRICH-iST, highlighting platelet, peripheral blood mononuclear cell, and erythrocyte markers.** *A* and *B,* Mean quantification values of each protein in SD and ZDF rat plasma samples prepared using Mag-Net and ENRICH-iST were used to generate the ranking plot. The median rankings of the platelet, peripheral blood mononuclear cell, and erythrocyte markers were 95, 357, and 1501 in Mag-Net, and 105, 317, and 1078 in ENRICH-iST, respectively. The top five proteins for each cell type are highlighted. peripheral blood mononuclear cell; ZDF, Zucker Diabetic Fatty.

(Supplemental Table S4). Both the contamination indices and enrichment scores for platelets were elevated by one order of magnitude, corresponding to an estimated contamination level of 1 to 4.0 $\times$ 10^5 cells/μl plasma, as described by Korff *et al.* (17). Importantly, these metrics alone cannot distinguish between contamination by intact platelets and enrichment of platelet-derived extracellular vesicles (PEVs) and may therefore contribute to apparent increases in platelet-associated markers. To further clarify these findings, we sought to refine our interpretation by integrating additional data, including Simple Western and nanoparticle tracking analysis (NTA).

To confirm EV enrichment from rat plasma, Mag-Net samples were analyzed using Simple Western blotting. Cd9 was detected in the Mag-Net sample prepared from 100 μl of plasma but not from 20 μl, likely due to its low abundance or low antibody reactivity (Supplemental Fig. S12). In contrast, Cd63, Cd81, and Tsg101 were detected in both Mag-Net samples (Supplemental Figs. S13–S15). Notably, Flot1 was detected in both plasma and Mag-Net samples but was not detected in the PPP sample processed by additional centrifugation (2500 g $\times$ 15 min, 20 °C) (Supplemental Fig. S16). On the other hand, although Alix was strongly detected in both Mag-Net samples, it was also detected in both plasma and PPP samples (Supplemental Fig. S17). Conversely, the abundances of typical plasma contamination markers such as Alb and Apoa1 were reduced in Mag-Net samples (Supplemental Figs. S18 and S19). NTA also confirmed the enrichment of small EVs by the Mag-Net method (Supplemental Fig. S20). The particle concentration was 7.45 $\times$ 10^{11} particles/ml, which is two orders of magnitude higher than values reported in previous studies using the Mag-Net method (4, 7). The most frequent and mean size of particles were 67.5 nm and 94 nm, respectively.

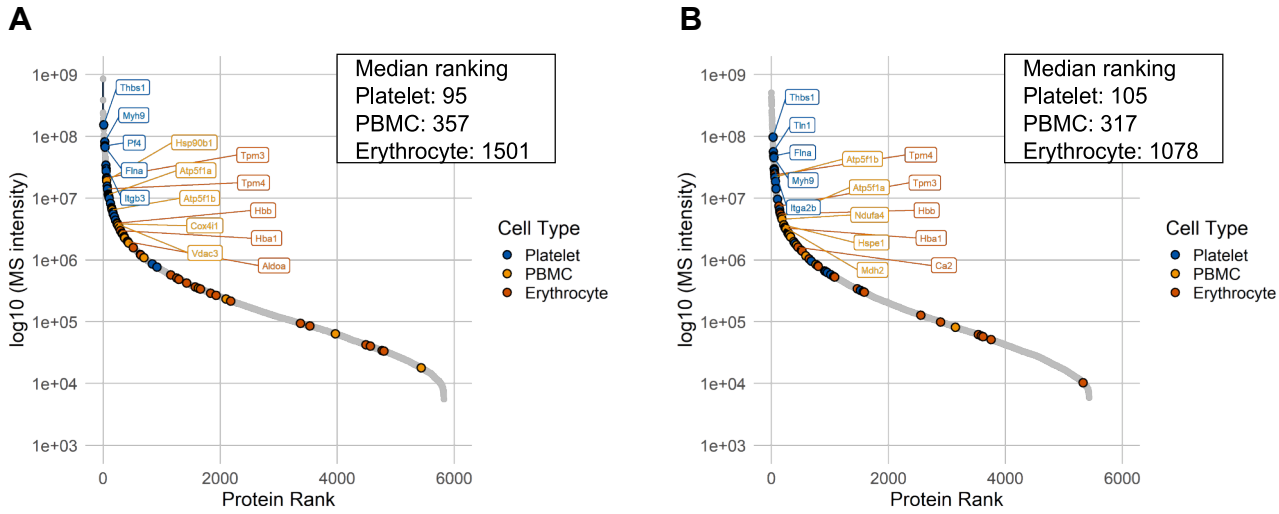

FIG. 7. **Enrichment of tissue-specific proteins.** *A,* identified tissue-specific proteins in Mag-Net and ENRICH-iST samples. *B,* liver/brain-specific proteins that exhibited more than ten-fold higher mean quantification values in the Mag-Net compared to the ENRICH-iST.

Deregulated Pathways in ZDF Rats Compared to SD Rats

IPA was carried out on sets of 219-down and 80-upregulated proteins (fold change $\geq$ 1.5, $p_{BH} \leq 0.05$) which were identified with the Mag-Net method (Fig. 8*A*) while sets of 68-down and 43-upregulated proteins (fold change $\geq$ 1.5, $p_{BH} \leq 0.2$) were identified with the ENRICH-iST method (Fig. 8*B*) (Supplemental Table S1). Stricter criteria (fold change $\geq$ 1.5, $p_{BH} \leq 0.05$) were not applied to the ENRICH-iST samples, since only small sets of 10-down and 5-upregulated proteins were identified (Supplemental Fig. S21). IPA cannot be performed on such a limited number of proteins, as the recommended number of genes for IPA is 100–3000 according to the latest IPA manual (Qiagen Knowledge Base, Summer 2025: https://qiagen.my.salesforce-sites.com/KnowledgeBase?id=kA41i000000L5p6CAC).

All significantly deregulated pathways were identified as downregulated pathways (Fig. 9, *A* and *B*). Some of the significantly downregulated pathways (*e.g.,* elastic fiber formation and integrin cell surface interactions) were uniquely identified by the Mag-Net method (Fig. 9*A*). Most pathways that were significantly downregulated in ZDF rats and identified by the ENRICH-iST method (*e.g.,* collagen biosynthesis and modifying enzymes) were also covered by the Mag-Net method (Fig. 9*B*). Although $p_{BH} \leq 0.2$ is too loose as statistical threshold, IPA of

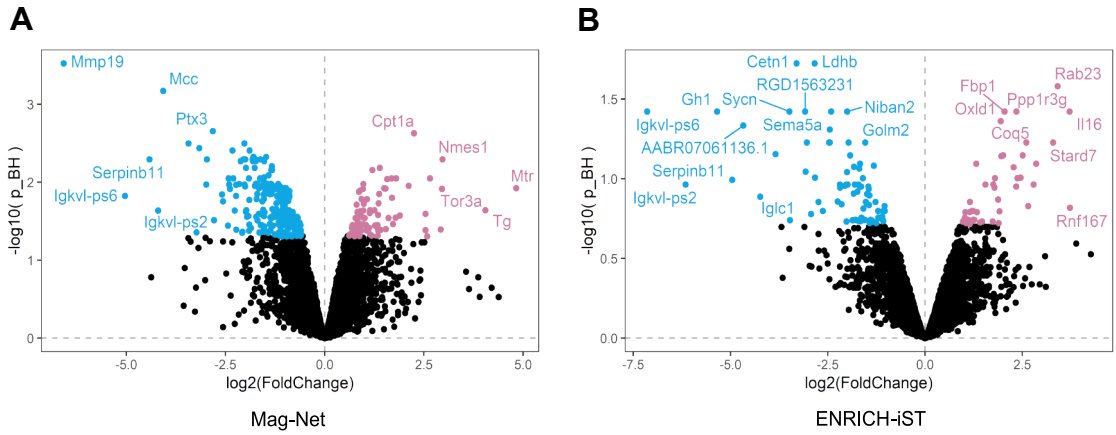

FIG. 8. **Volcano plot showing deregulated proteins in Mag-Net and ENRICH-iST samples.** Log2-transformed intensity ratios of proteins quantified in plasma samples from SD and ZDF rats were visualized using IPA. *Pink* and *blue colors* indicate proteins that were significantly upregulated and downregulated, respectively, in ZDF rats compared with SD rats. *A,* a total of 219 downregulated and 80 upregulated proteins were identified in Mag-Net samples using the criteria (fold change $\geq$ 1.5, $p_{BH} \leq 0.05$). *B,* a total of 68 downregulated and 43 upregulated proteins were identified in ENRICH-iST samples using the criteria (fold change $\geq$ 1.5, $p_{BH} \leq 0.2$). SD, Sprague-Dawley; ZDF, Zucker Diabetic Fatty.

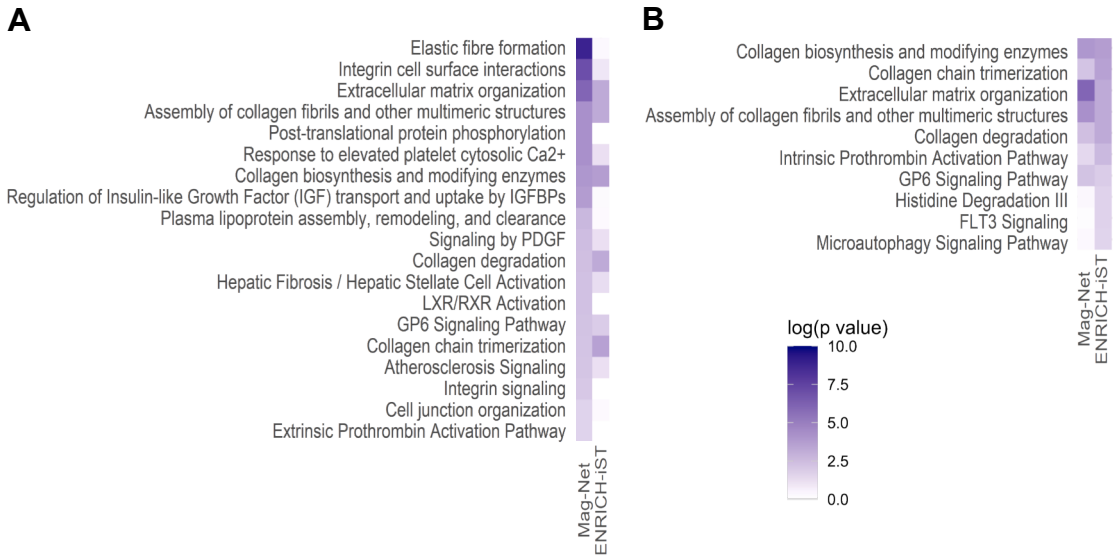

FIG. 9. **Significantly deregulated pathways identified by IPA.** *A,* comparison analysis sorted by Mag-Net. *B,* comparison analysis sorted by ENRICH-iST. Not significant (p-value > 0.001) pathways in the method used for sorting are not shown. No upregulated pathway was identified. The deregulated protein number was different among methods (299 *versus* 111 in Mag-Net and ENRICH-iST, respectively).

Mag-Net and ENRICH-iST dataset under the same criteria (fold change ≥ 1.5, $p_{BH} \leq 0.2$) was also performed and similar result was confirmed (Supplemental Fig. S22).

Comparison of Short-Gradient Orbitrap Astral and Long-Gradient Orbitrap Fusion Lumos for Plasma Proteomics

An Orbitrap Astral mass spectrometer with a 42.6-min gradient was preliminarily evaluated for high-throughput analysis using the remaining Mag-Net technical replicates of control rat plasma, with 500 ng of peptides injected into the LC-MS (Supplemental Methods & Figures). After removing proteins detected in fewer than two out of three replicates, a total of 5508 proteins were identified (Supplemental Table S1). Among these, 5146 proteins overlapped with the dataset obtained using an Orbitrap Fusion Lumos mass spectrometer with a 125-min gradient (Fig. 10). The shorter gradient also identified 342 tissue-specific proteins, of which 313 overlapped with those identified by the 125-min method (Fig. 10). Achieving approximately 90% of the identifications from the long-gradient method for both total and tissue-specific proteins, while increasing throughput about three-fold, represents a well-balanced compromise.

DISCUSSIONS

Prior to the evaluation of Mag-Net and ENRICH-iST, the Mag-Net protocol was optimized based on version four of the protocol. The latest version five protocol (https://resynbio.com/wp-content/uploads/2023/12/Mag-Net-EV-Manual-Enrichment-Ver5.pdf) was also investigated using 20 µl of healthy control SD3 rat plasma but it provided one-fifth recovery of digested peptides (Supplemental Fig. S23). PreOmics recently released a new version of ENRICH-iST kit, ENRICHplus, however, this study focused on ENRICH-iST method because the ENRICHplus method requires 50 µl as the lowest starting plasma volume (6, 27). Analysis of missed tryptic cleavages revealed that fewer missed cleavages were associated with an

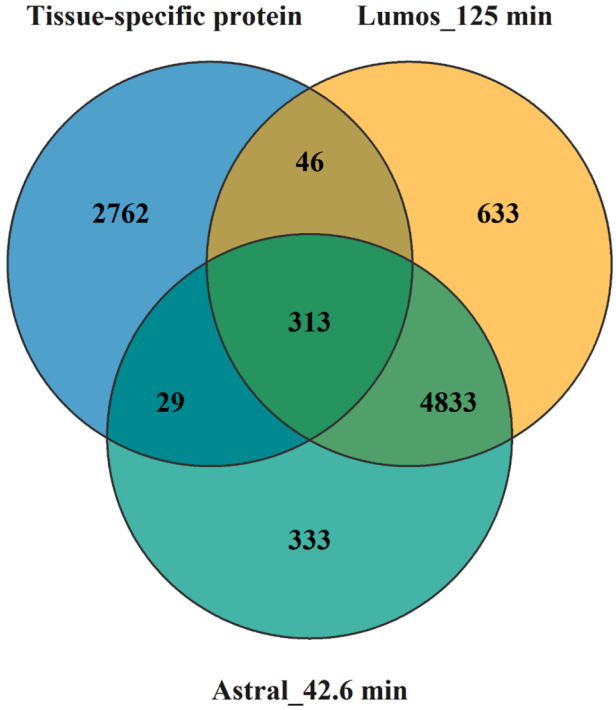

FIG. 10. **Comparison of short-gradient Orbitrap Astral and long-gradient Orbitrap Fusion Lumos.** Overlap of tissue-specific proteins and Mag-Net–identified proteins obtained using the Astral 42.6-min and Lumos 125-min methods.

increased number of identified proteins (Supplemental Fig. S1). Although on-beads digestion has the advantage of minimizing sample loss, it has the drawback of higher missed cleavage rates compared to in-solution digestion. By changing the trypsin digestion to an overnight incubation, missed cleavage was reduced, which likely contributed to an increase in the number of identified proteins and a decrease in variability of quantitative values. In addition to the minimum required starting plasma volume, a high-throughput workflow is important for large scale plasma proteomics. For sample preparation, the automation of both the Mag-Net (28) and ENRICH-iST (https://www.preomics.com/products/enrich-ist, accessed on 18th June 2025) methods have been reported. In contrast to Mag-Net, ENRICH-iST requires transferring the sample solution to a cartridge during desalting and then to a collection plate after purification. This workflow involves moving cartridges between 96-well plates, necessitating an automated system equipped with a gripper, such as the Agilent Bravo platform. Gripper-equipped systems are generally more complex to operate than the KingFisher system; therefore, it is recommended to follow application notes for each system when developing scripts. From a cost perspective, ENRICH-iST is a ready-to-use commercial kit that incurs additional expenses compared to Mag-Net. Mag-Net therefore offers potential cost advantages, particularly for large-scale applications. When the trypsin digestion time is set to overnight for both methods, 96 samples can be prepared within 24 h. Therefore, the practical bottleneck for throughput lies not in the sample preparation method but in the LC-MS measurement time. Our evaluation of high-throughput analysis using Orbitrap Astral with a short LC gradient demonstrated that approximately 90% of the protein identifications obtained with the long-gradient method can be achieved while increasing the throughput by at least three-fold. However, this was based on a preliminary setup without extensive LC-MS method optimization. Therefore, further refinement of the LC-MS conditions could potentially enhance throughput and maintain or even improve proteome coverage.

Despite having different mechanisms, the Mag-Net and ENRICH-iST approaches showed a substantial overlap in protein identifications and quantifications. This degree of overlap is expected, as eliminating highly abundant plasma proteins is inherently challenging, and both approaches are enrichment-based rather than absolute purification. Therefore, the presence of many shared abundant proteins in both datasets is not surprising. However, beyond this shared baseline, clear differences between the two approaches emerged. Mag-Net consistently outperformed ENRICH-iST in both proteome coverage and reproducibility, as evidenced by the higher number of identified proteins and the lower coefficients of variation.

Several factors may explain why Mag-Net outperforms ENRICH-iST in reproducibility and coverage, which can be broadly attributed to both physicochemical and methodological aspects. Mag-Net enables single-pot sample preparation through membrane particle capture and on-bead tryptic digestion, minimizing protein and peptide losses by reducing transfers and maintaining all steps within the same tube or well. In contrast, ENRICH-iST involves multiple transfers during desalting and purification, which may lead to peptide loss; if this is the case, adding surfactants such as lauryl maltose neopentyl glycol could help mitigate the issue (29).

The difference in missed cleavage variability likely reflects the digestion protocol: Mag-Net employs overnight digestion, allowing the proteolytic reaction to reach completion and stabilize variability, whereas ENRICH-iST uses a 1-h digestion, resulting in greater sample-to-sample variation (Supplemental Table S1). The slightly higher missed cleavage rate in Mag-Net may relate to non-enzymatic modifications during prolonged incubation, although this remains speculative. Additionally, Mag-Net's size-based netting capture by MagReSyn beads could limit trypsin accessibility to certain proteins. While higher missed cleavage typically indicates incomplete digestion, it can occasionally improve protein coverage by generating partially cleaved peptides that expand sequence representation.

Mag-Net showed clearer clustering within each group in PCA, except for SD2 sample. Especially for the Mag-Net protocol to enrich membrane-associated particles, the handling of plasma samples including blood collection should follow the Minimal Information for Studies of Extracellular Vesicles guidelines (30). Repeated freezing/thaw cycle of SD2 plasma possibly affected the stability of membrane particles enriched by the Mag-Net method. To assess the quality of SD2 sample, we evaluated the reproducibility among the control samples by examining the number of identified proteins, the correlation coefficients of protein abundances, and the proteins that strongly contributed to PC2 in the PCA. These results indicate that SD2 was comparable to SD1 and SD3, however, the SD2 control sample may be excluded if other suitable samples are available. Nevertheless, in practice, testing often needs to proceed even when samples of variable quality are included. The Mag-Net method has been proposed as a sensitive and robust approach that remains applicable under such challenging conditions. Besides, in comparison to tissue proteomics, plasma proteomics is generally associated with greater variability in quantitative values, which poses challenges in identifying statistically significant differentially, expressed proteins. However, the Mag-Net method allows for very clear identification of such proteins due to its low variability in quantitative measurements.

EV enrichment from rat plasma by the Mag-Net method was confirmed using Simple Western blotting and NTA (Supplemental Figs. S12–S20). Cd9 was not detected in the Mag-Net sample prepared from 20 μl plasma, likely due to its low abundance or low antibody reactivity; therefore, the Mag-Net sample prepared from 100 μl plasma was additionally

measured. In contrast, Cd63, Cd81, and Tsg101 were detected in both Mag-Net samples. Importantly, Flot1 was detected in the plasma sample as well as in the Mag-Net samples. However, it was not detected in the PPP sample processed by an additional centrifugation (2500 g × 15 min, 20 °C). Although platelet-derived small EVs are not pelleted at 2500×*g*, larger platelet-derived microvesicles are efficiently removed by this centrifugation step. Flot1 is categorized as "2a: with lipid or membrane protein-binding ability" in the Minimal Information for Studies of Extracellular Vesicles guidelines (30), which differs clearly from endosomal sorting complex required for transport-associated proteins such as Tsg101 and Alix. This property explains the disappearance of the Flot1 signal in PPP sample after additional centrifugation. In contrast, the Alix band was only minimally reduced in PPP, supporting the presence of platelet-derived small EVs rather than contamination by intact platelets. Alix is rarely detected at high levels in plasma containing intact platelets, making this interpretation consistent with the observed Simple Western immunoblotting pattern. The elevated EV concentration of 7.45×10^{11} particles/ml determined by NTA (Supplemental Fig. S20) is also indicative of potential enrichment of platelet-derived small EVs. Considering that platelet activation is enhanced in diabetes (31), focusing on changes in PEVs may be particularly relevant in the context of ZDF rats. Thus, although PEVs can represent a confounding factor in other disease settings by masking biologically relevant signals, they may constitute a biologically informative EV population in diabetes research.

Korff *et al.* have previously cautioned that bead-based approaches enhance the detection of low-abundance proteins but are more vulnerable to systematic bias when applied to non-ideal specimens (17). To address this issue, their three-step quality control strategy is useful: (i) assessing contamination in individual samples using validated marker panels and excluding outliers relative to study-specific baselines, (ii) detecting potential bias between study groups, and (iii) correlating candidate biomarkers with cell-specific markers using global correlation maps to identify artifacts and distinguish genuine biological signals from technical effects. In the present study, this framework was complemented by independent assessments using Simple Western and NTA to evaluate sample quality and potential contamination. Importantly, no outlier samples and no systematic bias between groups were identified by contamination assessment (Supplemental Table S4), thereby preserving the validity of comparative analyses, even in the absence of step 3 correlation analyses. Notably, pathways involving elastin and collagen—proteins that are not known to be major components of blood cell proteomes—were clearly detected, indicating the ability of the enrichment workflow to capture extracellular matrix–related alterations that would not be expected to arise from platelet carryover alone. In addition, integrin-associated pathways were also enriched by the Mag-Net method, despite the broad expression of integrins across various cell types and the substantial presence of PEVs. This observation suggests that the workflow can sensitively resolve subtle, disease-associated changes even under conditions of high PEV background. Together, these findings demonstrate that the optimized Mag-Net workflow retains sufficient analytical sensitivity and robustness to detect biologically meaningful protein differences in minimally processed plasma. Therefore, while residual PEV background represents an inherent limitation of plasma EV analyses, its consistent magnitude across samples, combined with the preservation of key biological signatures, supports the reliability of the conclusions drawn from this study.

As a note of caution, 1 M NaCl was used to elute intact EVs from magnetic beads for Simple Western and NTA, whereas on-beads digestion was performed for proteomics. This difference in procedure may lead to slight variations in the types and amounts of proteins recovered. In contrast, ENRICH-iST samples were not analyzed by Simple Western or NTA, as the ENRICH-iST method was not originally designed to enrich EVs and lacks a step for collecting intact EVs. On the other hand, it was not feasible to detect Cd9 in plasma by LC-MS-based proteomics due to the dynamic range issue (5, 32). According to a previous report, abundances of ALB and cell membrane proteins in human plasma differ by 10^6-fold (2). Nevertheless, the abundances of Alb and Cd9 in the samples enriched by Mag-Net and ENRICH-iST methods were within two-fold differences (Supplemental Fig. S11), indicating a certain enrichment of membrane-associated particles by Mag-Net and low-abundance proteins by ENRICH-iST, respectively. Given that the mechanism of ENRICH-iST enrichment is not disclosed, understanding its specificity and limitations is essential. Our findings indicate that ENRICH-iST preferentially captures proteins associated with extracellular regions (Supplemental Figs. S8 and S9), suggesting its suitability for analyzing classical secreted proteins that are not incorporated into EVs.

Enrichment of tissue-derived EVs from body fluids is an emerging technology to monitor the tissue-specific changes without tissue biopsy (1, 33). More than half of the tissue-specific proteins were classified as being specific to either the liver or the brain tissues. Among them, brain tissue-specific proteins (Cnp, Llgl1, Mbp, Nrgn, Rab3a, Ywhah) involved in PPI previously reported by Muraoka (1) were identified in Mag-Net samples as well. Of these, only Nrgn was significantly increased in ZDF rats (Supplemental Fig. S24), but other five proteins were not deregulated. The ability to monitor them through plasma samples is very appealing because Nrgn and Ywhah have been identified as promising biomarkers for prediction of cognitive resilience versus decline in Alzheimer's disease (34, 35). Proz and Serpina10 were highly enriched in Mag-Net samples as liver tissue-specific proteins involved in PPI. Interestingly, Proz was significantly upregulated in ZDF rats (Supplemental

Fig. S25), which indicates the anti-inflammatory and cardiovascular-protective function of Proz (36). Furthermore, Cyp8b1 was detected only in Mag-Net samples and significantly upregulated in ZDF rats (Supplemental Fig. S26). Although Cyp8b1 belongs to the Cytochrome P450 (CYP) family, it functions as a bile-acid–synthesizing enzyme rather than a classical drug-metabolizing CYP (37). Therefore, the well-known strain differences reported for major drug-metabolizing CYPs (38, 39) are less applicable to Cyp8b1. Given that Cyp8b1 is primarily expressed in the liver and rarely observed in circulation, its increased abundance in plasma is noteworthy and suggests that plasma proteomics can capture liver-specific metabolic alterations associated with disease progression, highlighting its potential as a non-invasive biomarker source. Moreover, reduction or inhibition of Cyp8b1 can be an approach to improve glucose homeostasis (40, 41).

In this study, healthy SD rats were used as a reference group, although lean ZDF rats would have been a more appropriate control model for comparison with ZDF rats, as SD rats are not genetically matched. It is desirable to conduct biomarker discovery for diabetes again using an experimental system with a unified genetic background for validation. However, focusing on drug-metabolizing proteins such as CYP, UDP-glucuronosyltransferase, sulfotransferase, and transporter, which are well known to exhibit pronounced strain differences (38, 39), none of these were included in the pathways identified by IPA. These results suggest that disease-related differences exert a stronger influence on pathway analysis than genetic variability. Indeed, the deregulated proteins and pathways identified in ZDF rats through IPA appeared to be reasonably associated with diabetes. The pathway "collagen biosynthesis and modifying enzymes" was identified as the most significantly downregulated in the ENRICH-iST samples. It is known that collagen production is decreased in diabetic rats (42). Whereas the two most significantly downregulated pathways, "elastic fiber formation" and "integrin cell surface interactions", were identified only in the Mag-Net samples. Elastin is a fundamental protein to maintain the elasticity of blood vessels (43). Decrease of elastin in diabetes has been reported in tissue (44), however, never reported in plasma, showcasing the advantages of Mag-Net protocol as a liquid biopsy proteomics. Integrin involves various functions such as cell-to-cell adhesion and cell signaling (45). Besides, antibodies that mask the binding sites of CD11a or its ligand ICAM-1 can reduce dendritic cell uptake of EV so that it affects the immune response (46, 47).

In conclusion, this study shows that the Mag-Net method provides deeper proteome coverage and higher precision than ENRICH-iST using only 20 μl of rat plasma. While both methods identified more than 5000 proteins, Mag-Net more effectively captured EV-associated signatures and revealed a larger number of deregulated proteins and unique pathways, including elastic fiber formation, in type 2 diabetic rats. These findings highlight Mag-Net as a robust and broadly applicable approach for small-volume plasma proteomics, supporting its utility in biomarker discovery and non-clinical drug evaluation.

DATA AVAILABILITY

The proteomics data have been deposited in the ProteomeXchange Consortium via the jPOST repository (48) under the dataset identifiers PXD067811 (ProteomeXchange) and JPST003978 (jPOST).

Supplemental data—This article contains supplemental data.

Acknowledgments—Authors thank Kaori Makino and Aya Mizobuchi for sample preparations and supporting NTA. Authors also thank Keiichi Kami for supporting Simple Western analysis. The graphical abstract was created using materials provided by PreOmics, Resyn Biosciences, and Thermo Fisher Scientific.

Author Contribution—R. T., F. P., and A. M. writing–review and editing; R. T. writing–original draft; R. T. and F. P. visualization; R. T. methodology; R. T. investigation; R. T. and F. P. formal analysis; R. T. conceptualization; A. K. supervision.

Funding and Additional Information—The study was funded by Boehringer Ingelheim GmbH.

Conflict of Interest—The authors declare no competing interests.

Abbreviations—The abbreviations used are: Alb, albumin; Alix, ALG-2-interacting protein X; Apoa1, apolipoprotein A1; CYP, Cytochrome P450; DIA, data-independent acquisition; EV, extracellular vesicle; Flot1, flotillin-1; GO, gene ontology; IPA, Ingenuity Pathway Analysis; NTA, nanoparticle tracking analysis; PBMC, peripheral blood mononuclear cell; PCA, Principal component analysis; PEV, platelet-derived extracellular vesicle; PPI, protein-protein interaction; PPP, platelet-poor-plasma; SAX, strong anion exchange; Tsg101, tumor susceptibility gene 101 protein; ZDF, Zucker Diabetic Fatty.

Received September 9, 2025, and in revised form, April 19, 2026
Published, MCPRO Papers in Press, May 20, 2026, https://doi.org/10.1016/j.mcpro.2026.101591

REFERENCES

1. Muraoka, S., Hirano, M., Isoyama, J., Nagayama, S., Tomonaga, T., and Adachi, J. (2022) Comprehensive proteomic profiling of plasma and serum phosphatidylserine-positive extracellular vesicles reveals tissue-specific proteins. *iScience* **25**, 104012
2. Geyer, P. E., Holdt, L. M., Teupser, D., and Mann, M. (2017) Revisiting biomarker discovery by plasma proteomics. *Mol. Syst. Biol.* **13**, MSB156297
3. Metatla, I., Roger, K., Chhuon, C., Ceccacci, S., Chapelle, M., Schmit, P.-O., *et al*. (2024) Neat plasma proteomics: getting the best out of the worst. *Clin. Proteom.* **21**, 22

4. Suresh, P. S., and Zhang, Q. (2025) Comprehensive comparison of methods for isolation of extracellular vesicles from human plasma. *J. Proteome Res.* **24**, 2956–2967
5. [preprint] Wu, C. C., Tsantilas, K. A., Park, J., Plubell, D., Sanders, J. A., Naicker, P., *et al*. (2024) Mag-Net: rapid enrichment of membrane-bound particles enables high coverage quantitative analysis of the plasma proteome. *BioRxiv*. https://doi.org/10.1101/2023.06.10.544439
6. Beimers, W. F., Overmyer, K. A., Sinitcyn, P., Lancaster, N. M., Quarmby, S. T., and Coon, J. J. (2025) Technical evaluation of Plasma Proteomics Technologies. *J. Proteome Res.* **24**, 3074–3087
7. Wu, C. C., Tsantilas, K. A., Park, J., Plubell, D., Sanders, J. A., Naicker, P., *et al*. (2025) Enrichment of extracellular vesicles using Mag-Net for the analysis of the plasma proteome. *Nat. Commun.* **16**, 5447
8. Skandalou, E., Rivedal, M., Marti, H.-P., Halden, T. A. S., Jenssen, T., Vikse, B. E., *et al*. (2025) Proteome of renal tubuli and Serum differentiate pre-existing type 2 diabetes and post-transplant diabetes in kidney transplant recipients. *Proteom. Clin. Appl.* **19**, e70000
9. Shanbhag, S., Al-Sharabi, N., Fritz-Wallace, K., Kristoffersen, E. K., Bunæs, D. F., Romandini, M., *et al*. (2024) Proteomic analysis of human serum proteins adsorbed onto collagen barrier membranes. *J. Funct. Biomater.* **15**, 302
10. Demichev, V., Messner, C. B., Vernardis, S. I., Lilley, K. S., and Ralser, M. (2018) DIA-NN: neural networks and interference correction enable deep proteome coverage in high throughput. *Nat. Methods* **17**, 41–44
11. Tyanova, S., Temu, T., and Cox, J. (2016) The MaxQuant computational platform for mass spectrometry-based shotgun proteomics. *Nat. Protoc.* **11**, 2301–2319
12. Tyanova, S., Temu, T., Sinitcyn, P., Carlson, A., Hein, M. Y., Geiger, T., *et al*. (2016) The Perseus computational platform for comprehensive analysis of (prote)omics data. *Nat. Methods* **13**, 731–740
13. Sherman, B. T., Hao, M., Qiu, J., Jiao, X., Baseler, M. W., Lane, H. C., *et al*. (2022) DAVID: a web server for functional enrichment analysis and functional annotation of gene lists (2021 update). *Nucleic Acids Res.* **50**, W216–W221
14. Huang, D. W., Sherman, B. T., and Lempicki, R. A. (2009) Systematic and integrative analysis of large gene lists using DAVID bioinformatics resources. *Nat. Protoc.* **4**, 44–57
15. Krämer, A., Green, J., Pollard, J., and Tugendreich, S. (2013) Causal analysis approaches in Ingenuity Pathway Analysis. *Bioinformatics* **30**, 523–530
16. Szklarczyk, D., Kirsch, R., Koutrouli, M., Nastou, K., Mehryary, F., Hachilif, R., *et al*. (2023) The STRING database in 2023: protein-protein association networks and functional enrichment analyses for any sequenced genome of interest. *Nucleic Acids Res.* **51**, D638–D646
17. Korff, K., Müller-Reif, J. B., Fichtl, D., Albrecht, V., Schebesta, A.-S., Itang, E. C. M., *et al*. (2025) Pre-analytical drivers of bias in bead-enriched plasma proteomics. *EMBO Mol. Med.* **17**, 3174–3196
18. Keerthikumar, S., Chisanga, D., Ariyaratne, D., Saffar, H. A., Anand, S., Zhao, K., *et al*. (2016) ExoCarta: a web-based compendium of exosomal cargo. *J. Mol. Biol.* **428**, 688–692
19. Kyte, J., and Doolittle, R. F. (1982) A simple method for displaying the hydropathic character of a protein. *J. Mol. Biol.* **157**, 105–132
20. Wang, S., Lu, Z., Wang, Y., Zhang, T., and He, X. (2020) Metalloproteins and apolipoprotein C: candidate plasma biomarkers of T2DM screened by comparative proteomics and lipidomics in ZDF rats. *Nutr. Metab.* **17**, 66
21. Ben-Nissan, G., Katzir, N., Füzesi-Levi, M. G., and Sharon, M. (2022) Biology of the extracellular proteasome. *Biomolecules* **12**, 619
22. Henry, L., Gallic, L. L., Garcin, G., Coux, O., Jumez, N., Roger, P., *et al*. (2011) Proteolytic activity and expression of the 20S proteasome are increased in psoriasis lesional skin. *Br. J. Dermatol.* **165**, 311–320
23. Henry, L., Fabre, C., Guiraud, I., Bastide, S., Fabbro-Peray, P., Martinez, J., *et al*. (2013) Clinical use of p-proteasome in discriminating metastatic melanoma patients: comparative study with LDH, MIA and S100B protein. *Int. J. Cancer* **133**, 142–148
24. Martino, M., Hoetzenecker, K., Ankersmit, H. J., Roth, G. A., Haitel, A., Waldert, M., *et al*. (2012) Serum 20S proteasome is elevated in patients with renal cell carcinoma and associated with poor prognosis. *Br. J. Cancer* **106**, 904–908
25. Uhlén, M., Fagerberg, L., Hallström, B. M., Lindskog, C., Oksvold, P., Mardinoglu, A., *et al*. (2015) Tissue-based map of the human proteome. *Science* **347**, 1260419
26. Choi, Y., Park, J. H., Jo, A., Lim, C.-W., Park, J.-M., Hwang, J. W., *et al*. (2025) Blood-derived APLP1+ extracellular vesicles are potential biomarkers for the early diagnosis of brain diseases. *Sci. Adv.* **11**, eado6894
27. Roger, K., Metatla, I., Ceccacci, S., Wahbi, K., Motté, L., Chhuon, C., *et al*. (2025) Mining the plasma proteome: evaluation of enrichment methods for depth and reproducibility. *J. Proteom.* **321**, 105519
28. Järvinen, E., Liu, X., Varjosalo, M., and Keskitalo, S. (2025) Automated MagNet enrichment unlocks deep and cost-effective LC-MS plasma proteomics. *bioRxiv* **2025**
29. Konno, R., Ishikawa, M., Nakajima, D., Endo, Y., Ohara, O., and Kawashima, Y. (2024) Universal pretreatment development for low-input proteomics using Lauryl Maltose Neopentyl glycol. *Mol. Cell. Proteom* **23**, 100745
30. Welsh, J. A., Goberdhan, D. C. I., O'Driscoll, L., Buzas, E. I., Blenkiron, C., Bussolati, B., *et al*. (2024) Minimal information for studies of extracellular vesicles (MISEV2023): from basic to advanced approaches. *J. Extracell. Vesicles* **13**, e12404
31. Cai, Z., Wang, Y., Hu, S., Yuan, Q., Liu, J., Luo, C., *et al*. (2025) The efficacy of platelet-derived extracellular vesicles in the treatment of diabetic wounds: a systematic review and meta-analysis of animal studies. *Arch. Dermatol. Res.* **317**, 244
32. Newman, L. A., Useckaite, Z., and Rowland, A. (2022) Addressing MISEV guidance using targeted LC-MS/MS: a method for the detection and quantification of extracellular vesicle-enriched and contaminant protein markers from blood. *J. Extracell. Biol.* **1**, e56
33. Rodrigues, A. D., Dyk, M., Sorich, M. J., Fahmy, A., Useckaite, Z., Newman, L. A., *et al*. (2021) Exploring the use of serum-derived small extracellular vesicles as liquid biopsy to Study the induction of hepatic cytochromes P450 and organic anion transporting polypeptides. *Clin. Pharmacol. Ther.* **110**, 248–258
34. Oh, H. S.-H., Urey, D. Y., Karlsson, L., Zhu, Z., Shen, Y., Farinas, A., *et al*. (2025) A cerebrospinal fluid synaptic protein biomarker for prediction of cognitive resilience versus decline in Alzheimer's disease. *Nat. Med.* **31**, 1592–1603
35. Liu, W., Lin, H., He, X., Chen, L., Dai, Y., Jia, W., *et al*. (2020) Neurogranin as a cognitive biomarker in cerebrospinal fluid and blood exosomes for Alzheimer's disease and mild cognitive impairment. *Transl. Psychiatry* **10**, 125
36. Weiss, L., Uhrig, W., Kelliher, S., Szklanna, P. B., Prendiville, T., Comer, S. P., *et al*. (2024) Proteomic analysis of extracellular vesicle cargoes mirror the cardioprotective effects of rivaroxaban in patients with venous thromboembolism. *Proteom. Clin. Appl.* **18**, e202300014
37. Vlahcevic, Z. R., Eggertsen, G., Björkhem, I., Hylemon, P. B., Redford, K., and Pandak, W. M. (2000) Regulation of sterol 12alpha-hydroxylase and cholic acid biosynthesis in the rat. *Gastroenterology* **118**, 599–607
38. Zhou, X., Rougée, L. R. A., Bedwell, D. W., Cramer, J. W., Mohutsky, M. A., Calvert, N. A., *et al*. (2016) Difference in the pharmacokinetics and hepatic metabolism of antidiabetic drugs in Zucker Diabetic Fatty and sprague-dawley rats. *Drug Metab. Dispos.* **44**, 1184–1192
39. Nishiyama, Y., Nakayama, S. M. M., Watanabe, K. P., Kawai, Y. K., Ohno, M., Ikenaka, Y., *et al*. (2016) Strain differences in cytochrome P450 mRNA and protein expression, and enzymatic activity among Sprague Dawley, Wistar, Brown Norway and Dark Agouti rats. *J. Vet. Méd. Sci.* **78**, 675–680
40. Kaur, A., Patankar, J. V., Haan, W., Ruddle, P., Wijesekara, N., Groen, A. K., *et al*. (2014) Loss of Cyp8b1 improves glucose homeostasis by increasing GLP-1. *Diabetes* **64**, 1168–1179
41. Chevre, R., Trigueros-Motos, L., Castaño, D., Chua, T., Corlianò, M., Patankar, J. V., *et al*. (2018) Therapeutic modulation of the bile acid pool by Cyp8b1 knockdown protects against nonalcoholic fatty liver disease in mice. *FASEB J.* **32**, 3792–3802
42. Spanheimer, R. G., Umpierrez, G. E., and Stumpf, V. (1988) Decreased collagen production in diabetic rats. *Diabetes* **37**, 371–376
43. Sinha, A., and Vyavahare, N. R. (2013) High-glucose levels and elastin degradation products accelerate osteogenesis in vascular smooth muscle cells. *Diabetes Vasc. Dis. Res.* **10**, 410–419
44. Shemesh, S., Sidon, E., Kaisler, E., Sheinis, D., Velkes, S., Ohana, N., *et al*. (2017) Diabetes mellitus is associated with increased elastin fiber loss in

ligamentum flavum of patients with lumbar spinal canal stenosis: results of a pilot histological study. *Eur. Spine J.* **27**, 1614–1622
45. Aplin, A. E., Howe, A., Alahari, S. K., and Juliano, R. L. (1998) Signal transduction and signal modulation by cell adhesion receptors: the role of integrins, Cadherins, immunoglobulin-cell adhesion molecules, and selectins. *Pharmacol. Rev.* **50**, 197–263
46. Mulcahy, L. A., Pink, R. C., and Carter, D. R. F. (2014) Routes and mechanisms of extracellular vesicle uptake. *J. Extracell. Vesicles* **3**
47. Morelli, A. E., Larregina, A. T., Shufesky, W. J., Sullivan, M. L. G., Stolz, D. B., Papworth, G. D., *et al*. (2004) Endocytosis, intracellular sorting, and processing of exosomes by dendritic cells. *Blood* **104**, 3257–3266
48. Okuda, S., Yoshizawa, A. C., Kobayashi, D., Takahashi, Y., Watanabe, Y., Moriya, Y., *et al*. (2024) jPOST environment accelerates the reuse and reanalysis of public proteome mass spectrometry data. *Nucleic Acids Res.* **53**, D462–D467